

A Novel HMSM Photodetector with Resonant Cavity for Short Haul Communications

Xiying Chen^a, and Bahram Nabet, Fabio Quaranta^b, and Adriano Cola, and Marc Currie^c

- a) Electrical and Computer Engineering Dept., Drexel University, Philadelphia, PA 19104 USA
- b) Institute of Microelectronics, National Research Council (C.N.R-I.M.E.), Via Arnesano I-73100 Lecce, Italy
- c) Naval Research Laboratory, 4555 Overlook Ave. S.W., Washington, DC 20375, USA

Abstract — A novel RCE (resonant-cavity-enhanced) HMSM (Heterostructure Metal-Semiconductor-Metal) photodetector with $\text{Al}_{0.24}\text{Ga}_{0.76}\text{As}/\text{Al}_{0.9}\text{Ga}_{0.1}\text{As}$ distributed Bragg reflector is presented. The photocurrent spectrum shows a clear peak at 850 nm wavelength with full width at half maximum (FWHM) of around 30 nm. The top reflector is a delta modulation doped $\text{Al}_{0.76}\text{Ga}_{0.24}\text{As}$ that also acts as the barrier enhancement layer thus providing very low dark current values. I-V curve shows that there is a five-fold decrease in dark current, with bias less than 10V and a factor of two increase in photocurrent as a result of delta doping. Time response measurements gives a 3-dB bandwidth of about 33-GHz. Combination of low dark current, fast response, wavelength selectivity, and compatibility with high electron mobility transistors makes this device especially suitable for short haul communications purposes.

I. INTRODUCTION

In addition to their important application in vertical cavity surface emitting lasers (VCSEL), resonant cavities (RC's) have been exploited in the design of vertical photodetectors, such as p-i-n heterojunction photodiodes, Schottky barrier internal emission photodiodes, and quantum well infrared photodetectors [1]-[3]. Resonant-cavity-enhanced (RCE) photodetectors have attracted much attention in the past few years due to their potential in solving the trade off between high quantum efficiency and high speed while, at the same time, offering narrow spectral bandwidth detection useful in wavelength-division multiplexing (WDM) applications [4].

On the other hand, the trend towards monolithic optoelectronic integrated circuits (OEIC) motivates appreciable research activity directed towards the employment of planar photodetectors, which can be easily fabricated and are compatible with the FET process. Planar metal-semiconductor-metal photodetectors (MSM-PD's) are good candidates for such OEIC receivers [5]-[6]. The FET technology itself is strongly affected by progress in heterojunction-based devices that take

advantage of reduced dimensionality regime of conduction, the high electron mobility transistor (HEMT) being a prime example. This has motivated the development of heterojunctions based photodetectors that enjoy better conduction while being compatible with HEMT technology [5]. In particular, we have previously proposed AlGaAs/GaAs heterostructure metal-semiconductor-metal photodetectors (HMSM-PD's) that show much less dark current than conventional MSM due to both the two dimensional electron gas (2DEG) and the effect of barrier enhancement due to the wide-gap material [7]-[9].

A common problem with planar, as well as vertical, photodetectors is the trade-off between speed and quantum efficiency; in order to achieve a fast response from photodetectors, the depleted absorption region needs to be small for reduced path length, but this results in a decreased responsivity due to small absorption depth. Resonant cavity technique offers the possibility to balance such conflict between fast speed and sensitivity [10]. The photodetector presented in this paper employs a vertical resonance cavity for high-speed operation, the heterojunction that forms its top mirror, however, not only doubles as a barrier enhancement layer to reduce dark current but also is modulation doped to produce an internal electric field that aids in transport of photocarriers.

II. THEORETICAL ANALYSIS AND DEVICE STRUCTURE

A typical RCE photodetector is made of a Fabry-Perot cavity, with a mirror on each end, whose length determines the resonant frequency. In practice, the bottom mirror consists of quarter-wave stacks of two different suitable materials forming a distributed Bragg reflector (DBR). The top mirror can be the interface between the native semiconductor and air due to their large difference of

refractive index; here we use a delta-doped heterojunction to achieve better photon reflection as well as other important electronic functionalities. Fig.1 shows a simplified structure of our RCE photodetector, where L_1 is the non-absorbing barrier enhancement layer. Recirculation of photons from the top of this layer and the bottom DBR, allows a thin absorption layer L_2 to be used to minimize the response time without hampering the quantum efficiency. Here quantum efficiency (η) is defined as the ratio of absorbed to incident photons, which can be written as[4]:

$$\eta = (1 - R_1)(1 - e^{-\alpha L_2})(1 + R_2 e^{-\alpha L_2}) / \{1 - 2\sqrt{(R_1 R_2)} e^{-\alpha L_2} \cos(2\beta L + \Psi_1 + \Psi_2) + R_1 R_2 e^{-2\alpha L_2}\} \quad (1)$$

where $\beta L = \beta_1 L_1 + \beta_2 L_2$, R_1 and R_2 are the top and bottom mirror reflectivities, respectively, α is the absorption coefficient of the absorption layer, Ψ_1 and Ψ_2 are phase shifts introduced by top and bottom mirrors, and β_1 and β_2 are the propagation constants in these two materials. From this formula, quantum efficiency is maximized when high reflection from DBR is high and the condition $\cos(2\beta L + \Psi_1 + \Psi_2) = 1$ is satisfied.

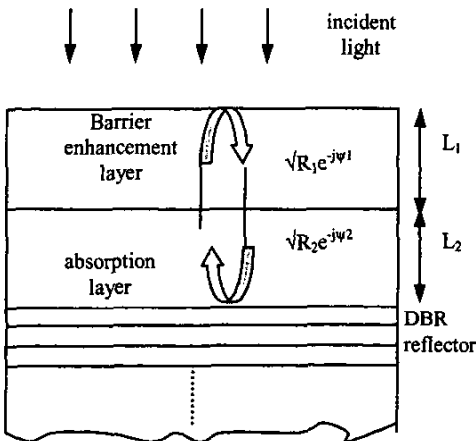


Fig. 1. Schematic diagram of the resonant-cavity-enhanced heterojunction photodetector. R_1 and R_2 are reflectivities and Ψ_1 and Ψ_2 are phase shifts introduced by the top and bottom mirrors, respectively.

There are three requirements for the materials to be selected to construct the bottom mirror: large refractive index difference, lattice matching to GaAs substrates, and bandgap larger than that of the active layer so that photons are not absorbed in the top layer. Based on their natural material properties, $\text{Al}_{0.24}\text{Ga}_{0.76}\text{As}$ and $\text{Al}_{0.9}\text{Ga}_{0.1}\text{As}$ are suitable pairs to construct this DBR-mirror [11]. The top mirror should reduce reflection from air and recirculate the

photons reflected from the bottom mirror. A 55 nm layer of $\text{Al}_{0.24}\text{Ga}_{0.76}\text{As}$ has been employed for this purpose, which also offers the following electronic properties. First, this layer lattice-matches to the absorption layer, with reduced DX-center defect levels due to low Al mole fraction, while providing surface stability. Second, it enhances the Schottky barrier between metal and GaAs due to its larger bandgap. Third, this layer is delta-doped to produce a 2DEG that is confined to the vicinity of the heterojunction by the conduction band discontinuity of about 0.3 eV. The last is the most important novel feature of this device. The confined electronic states of the quantum well at the interface as well as the electron cloud of the 2DEG have been shown to further enhance the barrier height and reduce the dark current, and thus the noise of these detectors [12]. This electron cloud is confined by a vertical electric field that has also been shown to aid in transport of photoelectrons [9]. Finally, modulation doping of this layer makes the growth compatible with HEMT. This top AlGaAs layer is delta doped, rather than uniformly, in order to take advantage of high channel electron density, reduced trapping effects, and improved threshold voltage as well as high breakdown characteristics [13]-[14].

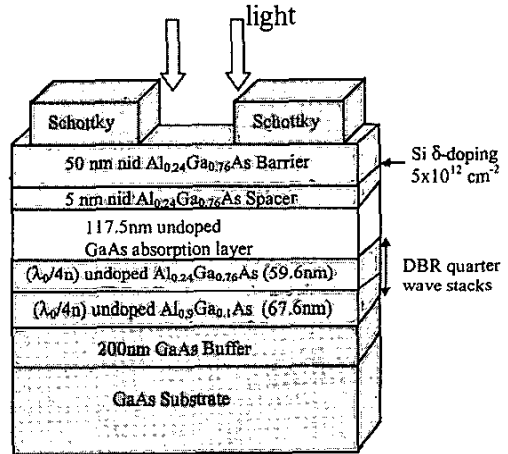


Fig. 2. Device structure of the resonant-cavity-enhanced HEMT photodetector.

A schematic cross-section of the grown RCE heterojunction MSM is shown in Fig. 2. The layer structure was grown by solid-source molecular beam epitaxy on a semi-insulating GaAs substrate. Twenty periods $\text{Al}_{0.24}\text{Ga}_{0.76}\text{As}/\text{Al}_{0.9}\text{Ga}_{0.1}\text{As}$ DBR were grown on a 200 nm GaAs buffer layer. The bottom mirror was designed for high reflectance at 830 nm center wavelength. The thickness of the top barrier enhancement layer is 50

nm and the spacer layer is 5 nm. A Si delta (δ) doped layer with sheet density of $5 \times 10^{12} \text{ cm}^{-2}$ was grown between barrier enhancement and spacer layers. The device area was $40 \times 40 \mu\text{m}^2$ with a typical interdigital pattern with finger width of 1 μm and distance of 4 μm .

A transmission line mode [4] was employed to design the layered structure and to simulate the optical properties of the RCE HMSCM photodetector. The thickness of the absorption layer, L_2 , is calculated by optimizing the quantum efficiency (1), which results in the condition $2\beta L + \Psi_1 + \Psi_2 = 2m\pi$. This condition is satisfied for integer values of m , with a higher number giving longer absorption length but slower response. A length $L_2 = 117.5$ nm was a satisfactory trade-off between speed and responsivity while still being only a fraction (11%) of the penetration depth.

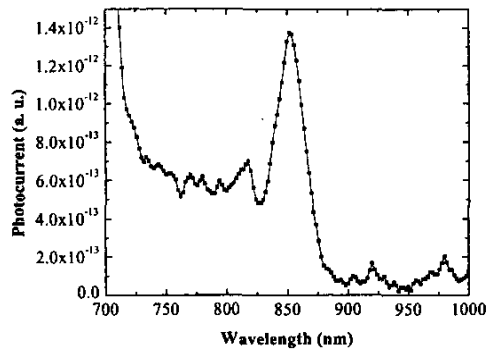


Fig. 3. Photocurrent spectral response of the resonant-cavity-enhanced HMSCM photodetector measured at 10V reverse bias.

III. RESULTS AND DISCUSSION

Fig. 3 shows the experimental photocurrent spectral response of the RCE-HMSCM photodetector. A monochromator with 0.15 nm resolution was used to select the excitation wavelength from a chopped tungsten light source. The signal was measured by a lock-in amplifier. The spectral response was measured under 10V reverse bias. The resonant peak value is around 850 nm not 830 nm possibly due to the angle of incidence of the single mode fiber optic line. The FWHM value is 30 nm. The shape of the photocurrent response, however, is asymmetric. This is due to the fundamental absorption edge of GaAs, which is around 870 nm and limits low energy absorption. Also, Fig. 3 is not normalized to

photon flux. A large increase in the photocurrent is observed around 710 nm, which is due to absorption in $\text{Al}_{0.24}\text{Ga}_{0.76}\text{As}$ layers.

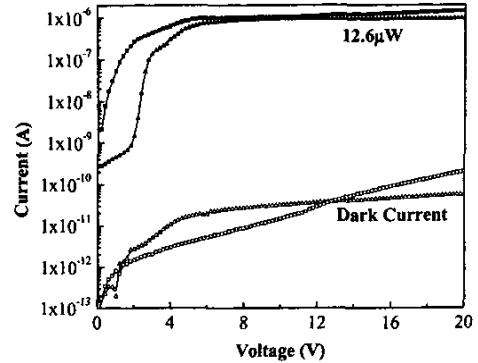


Fig. 4. Comparison of I-V behavior between the delta-doped and undoped devices with the identical structures. Δ : undoped device; $:$ doped device.

Fig. 4 shows the I-V curve of the dark current and photocurrent for two different devices. The only difference between the two devices is one does not have a doped plane in the wide gap material; this device is noted as undoped in figure caption. The mechanism responsible for around five times lower dark current in low bias in the delta-doped device can be the barrier enhancement due to electron-electron cloud interaction [12]. The vertical electric field and band bending potential profile in the direction of growth due to delta modulation doping as well conduction band discontinuity may cause a factor of two increase in photocurrent. Dark current of the device was around 15 picoamps at this bias, which normalizes to the very low value of 9.2 femtoamps/ μm^2 of device area, this making this device an excellent candidate for low noise operation.

High-speed time response measurements were made using a mode-locked Ti: Sapphire laser, operating at a repetition rate of 76 MHz that generated 100 fs pulses at a wavelength of 850 nm. Figure 5 shows the temporal response of a photodetector with a 1 μm finger and 4 μm spacing between fingers, measured by a 50 GHz sampling scope at 20 V bias. As seen in the figure, FWHM of the time response is 8.1 ps, its rise time is 8.8 ps, and fall time is 9 ps. Fourier transform of the data is shown in the inset of the figure and has a 3 dB (photocurrent) bandwidth of 33 GHz. The differential responsivity is 10.4 kV/W.

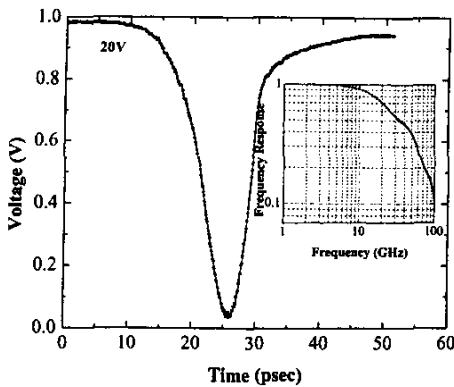


Fig. 5. Temporal response of the photodetector; insert shows the calculated frequency response.

IV. CONCLUSION

In conclusion, we have demonstrated a resonant-cavity-enhanced, heterostructure metal-semiconductor-metal photodetector operating around 850 nm. The device exhibited very low dark current wavelength channel selectivity, high quantum efficiency, and high-speed characteristics. Combination of low dark current, fast response, wavelength selectivity, and integrability with high electron mobility transistors makes this device especially suitable for short haul communications purposes.

ACKNOWLEDGEMENT

This work was partially supported by DARPA NGI program and by CNR through an STM award.

REFERENCES

- [1] E. Özbay, and İ. Kimukin, N. Biyikli, and O. Aytür, M. Gökkavas, G. Ulu, and M. S. Ünlü, R. P. Mirin, K. A. Bertness, and D. H. Christensen, "High-speed >90% quantum-efficiency p-i-n photodiodes with a resonance wavelength adjustable in the 795-835 nm range," *Appl. Phys. Lett.*, vol 74, no. 8, pp. 1072-1074, Feb. 1999.
- [2] İ. Kimukin, and E. Özbay, N. Biyikli, T. Kartaloglu, and O. Aytür, M. S. Ünlü, and G. Tuttle, "High-speed GaAs-based resonant-cavity-enhanced 1.3 μ m photodetector," *Appl. Phys. Lett.*, vol. 77, no. 24, pp.3890-3892, Dec. 2000.
- [3] A. Shen, H. C. Liu, M. Gao, E. Dupont, and M. Buchanan, J. Ehret, G. J. Brown, and F. Szmulowicz, "Resonant-cavity-enhanced p-type GaAs/AlGaAs quantum-well infrared photodetectors," *Appl. Phys. Lett.*, vol. 77, no. 15, pp. 2400-2402, Oct. 2000.
- [4] M. S. Ünlü, and S. Strite, "Resonant cavity enhanced photonic devices," *J. Appl. Phys.*, vol. 78, no. 2, pp. 607-639, July 1995.
- [5] J. H. Burroughes, "H-MESFET Compatible GaAs/AlGaAs MSM Photodetector," *IEEE Photonics Techno. Lett.*, vol. 3, no. 7, pp. 660-662, July 1991.
- [6] P. Fay, W. Wohlmuth, A. Mahajan, C. Caneau, S. Chandrasekhar, and I. Adesida, "A Comparative Study of Integrated Photoreceivers Using MSM/HEMT and PIN/HEMT Technologies," *IEEE Photonics Techno. Lett.*, vol. 10, no. 4, pp. 582-584, April 1998.
- [7] J. Culp, B. Nabet, F. Castro, and A. Anwar, "Intermediate temperature grown GaAs/AlGaAs photodetector with low dark current and high sensitivity," *Appl. Phys. Lett.*, vol. 73, no. 11, pp. 1562-1564, Sept. 1998.
- [8] B. Nabet, "A Heterojunction Metal-Semiconductor-Metal Photodetector," *IEEE Photonics Techno. Lett.*, vol. 9, no. 2, pp. 223-225, Feb. 1997.
- [9] B. Nabet, A. Cola, F. Quaranta, and M. Cesareo, R. Rossi, and R. Fucci, and A. Anwar, "Electron cloud effect on current injection across a Schottky contact," *Appl. Phys. Lett.*, vol. 77, no. 24, pp. 4007-4009, Dec. 2000.
- [10] Z. -M. Li, D. Landheer, M. Veilleux, D. R. Conn, R. Surridge, J. M. Xu, R. I. McDonald, "Analysis of a Resonant-Cavity Enhanced GaAs/AlGaAs MSM Photodetector," *IEEE Photonics Techno. Lett.*, vol. 4, no. 5, pp. 473-475, May 1992.
- [11] S. Adachi, "GaAs, AlAs, and Al_xGa_{1-x}As: Material parameters for use in research and device application," *J. Appl. Phys.*, vol. 58, no. 3, pp. R1-R29, August 1985.
- [12] A. Anwar, and B. Nabet, "Barrier enhancement mechanisms in heterodimensional contacts and their effect of current transport," *IEEE Trans. On Microwave Theory and Techniques*, vol. 50, no. 1, pp. 68-71, Jan. 2002.
- [13] N. Moll, M. R. Heuschen, and A. Fisher-Colbrie, "Pulse-Doped AlGaAs/InGaAs Pseudomorphic MODFET's," *IEEE Trans. Electron Devices*, vol. 35, no. 7, pp. 879-886, July 1988.
- [14] E. F. Schubert, "Delta doping of III-V compound semiconductors: Fundamentals and device applications," *J. Vac. Sci.*, vol. A8, no. 3, pp. 2980-2996, May/June 1990.